DOKUZ EYLÜL ÜNİVERSİTESİ MÜHENDİSLİK FAKÜLTESİ
FEN VE MÜHENDİSLİK DERGİSİ
Cilt/*Vol.*:17■No/*Number*:3■Sayı/*Issue*:51■Sayfa/*Page*:138-162■Eylül 2015/*September 2015*

Makale Gönderim Tarihi (PaperReceivedDate): 05.11.2015 Makale Kabul Tarihi (PaperAcceptedDate): 21.12.2015

FREE VIBRATION ANALYSIS OF TIMOSHENKO MULTI-SPAN BEAM CARRYING MULTIPLE POINT MASSES

(ÇOK SAYIDA TOPAKLANMIŞ KÜTLE TAŞIYAN ÇOK AÇIKLIKLI TIMOSHENKO KİRİŞİNİN SERBEST TİTREŞİM ANALİZİ)

Yusuf YEŞİLCE[1]

ABSTRACT

In this paper, the natural frequencies and mode shapes of Timoshenko multi-span beam carrying multiple point masses are calculated by using Numerical Assembly Technique (NAT) and Differential Transform Method (DTM). At first, the coefficient matrices for left-end support, an intermediate point mass, an intermediate pinned support and right-end support of Timoshenko beam are derived. Equating the overall coefficient matrix to zero one determines the natural frequencies of the vibrating system and substituting the corresponding values of integration constants into the related eigenfunctions one determines the associated mode shapes. After the analytical solution, DTM is used to solve the differential equations of the motion. The calculated natural frequencies of Timoshenko multi-span beam carrying multiple point masses for the different values of axial force are given in tables.

Keywords: Differential Transform Method, free vibration, intermediate point mass, natural frequency, Numerical Assembly Technique, Timoshenko multi-span beam

ÖZ

Bu çalışmada, çok sayıda topaklanmış kütle taşıyan Timoshenko kirişinin doğal frekansları ve mod şekilleri Nümerik Toplama Tekniği (NTT) ve Diferansiyel Transformasyon Metodu (DTM) kullanılarak hesaplanmıştır. İlk olarak, Timoshenko kirişinin sol uç mesnetinin, ara noktada topaklanmış kütlenin, ara mesnetin ve sağ uç mesnetin katsayılar matrisleri elde edilmiştir. Genel katsayılar matrisinin determinantı sıfıra eşitlenerek titreşen sistemin doğal frekansları hesaplanmış ve integrasyon sabitlerinin ilgili özdeğer fonksiyonlarında yerine yazılmasıyla aranan mod şekilleri elde edilmiştir. Analitik çözümden sonra, DTM kullanılarak diferansiyel hareket denklemleri çözülmüştür. Farklı eksenel kuvvet değerleri için çok sayıda topaklanmış kütle taşıyan Timoshenko kirişinin doğal frekans değerleri tablolar halinde sunulmuştur.

Anahtar Kelimeler: *Diferansiyel Transformasyon Metodu, serbest titreşim, ara noktalarda topaklanmış kütle, doğal frekans, Nümerik Toplama Tekniği, çok açıklıklı Timoshenko kirişi*

[1]Dokuz Eylül Üniversitesi, Mühendislik Fakültesi, İnşaat Mühendisliği Bölümü, İZMİR, yusuf.yesilce@deu.edu.tr (sorumlu yazar)

1. INTRODUCTION

The free vibration characteristics of the uniform or non-uniform beams carrying various concentrated elements (such as point masses, rotary inertias, linear springs, rotational springs, etc.) are an important problem in engineering. The situation of structural elements supporting motors or engines attached to them is usual in technological applications. The operation of machine and its free vibration may introduce severe dynamic stresses on the beam. Thus, a lot of studies have been published in the literature about the vibration characteristics of the uniform or non-uniform beams carrying concentrated elements.

Liu et al. [1] formulated the frequency equation for beams carrying intermediate concentrated masses by using the Laplace Transformation Technique. Wu and Chou [2] obtained the exact solution of the natural frequency values and mode shapes for a beam carrying any number of spring masses. Gürgöze and Erol [3, 4] investigated the forced vibration responses of a cantilever beam with a single intermediate support. Naguleswaran [5, 6] obtained the natural frequency values of the beams on up to five resilient supports including ends and carrying several particles by using Bernoulli-Euler Beam Theory and a fourth-order determinant equated to zero. Lin and Tsai [7] determined the exact natural frequencies together with the associated mode shapes for Bernoulli-Euler multi-span beam carrying multiple point masses. In the other study, Lin and Tsai [8] investigated the free vibration characteristics of Bernoulli-Euler multiple-step beam carrying a number of intermediate lumped masses and rotary inertias. The natural frequencies and mode shapes of Bernoulli-Euler multi-span beam carrying multiple spring-mass systems were determined by Lin and Tsai [9]. Wang et al. [10] studied the natural frequencies and mode shapes of a uniform Timoshenko beam carrying multiple intermediate spring-mass systems with the effects of shear deformation and rotary inertia. Yesilce et al. [11] investigated the effects of attached spring-mass systems on the free vibration characteristics of the 1-4 span Timoshenko beams. In the other study, Yesilce and Demirdag [12] described the determination of the natural frequencies of vibration of Timoshenko multi-span beam carrying multiple spring-mass systems with axial force effect. Lin [13] investigated the free and forced vibration characteristics of Bernoulli-Euler multi-span beam carrying a number of various concentrated elements. Yesilce [14] investigated the effect of axial force on the free vibration of Reddy-Bickford multi-span beam carrying multiple spring-mass systems. Lin [15] investigated the free vibration characteristics of non-uniform Bernoulli-Euler beam carrying multiple elastic-supported rigid bars.

DTM was applied to solve linear and non-linear initial value problems and partial differential equations by many researches. The concept of DTM was first introduced by Zhou [16] and he used DTM to solve both linear and non-linear initial value problems in electric circuit analysis. In the other study, the out-of-plane free vibration analysis of a double tapered Bernoulli-Euler beam, mounted on the periphery of a rotating rigid hub is performed using DTM by Ozgumus and Kaya [17]. Çatal [18, 19] suggested DTM for the free vibration analysis of both ends simply supported and one end fixed, the other end simply supported Timoshenko beams resting on elastic soil foundation. Çatal and Çatal [20] calculated the critical buckling loads of a partially embedded Timoshenko pile in elastic soil by DTM. Free vibration analysis of a rotating, double tapered Timoshenko beam featuring coupling between flapwise bending and torsional vibrations is performed using DTM by Ozgumus and Kaya [21]. In the other study, Kaya and Ozgumus [22] introduced DTM to analyze the free vibration response of an axially loaded, closed-section composite Timoshenko beam which features material coupling between flapwise bending and torsional vibrations due to ply orientation. For the first time, Yesilce and Catal [23] investigated the free vibration analysis of a one fixed, the other end simply supported Reddy-Bickford beam by using DTM in the other study. Since previous studies have shown DTM to be an efficient tool, and it has been applied to solve boundary value problems for many linear, non-linear integro-differential and differential-difference equations that are very important in fluid mechanics, viscoelasticity, control theory, acoustics, etc. Besides the variety of the problems to that DTM may be applied, its accuracy and simplicity in calculating the natural frequencies and plotting the mode shapes makes this method outstanding among many other methods.

In the presented paper, we describe the determination of the exact natural frequencies of vibration of the uniform Timoshenko multi-span beam carrying multiple point masses with axial force effect by using NAT and DTM. The natural frequencies of the beams are calculated, the first five mode shapes are plotted and the effects of the axial force and the influence of the shear are investigated by using the computer package, Matlab. Unfortunately, a suitable example that studies the free vibration analysis of Timoshenko multi-span beam carrying multiple point masses with axial force effect using NAT and DTM has not been investigated by any of the studies in open literature so far.

2. THE MATHEMATICAL MODEL AND FORMULATION

A Timoshenko uniform beam supported by h pins by including those at the two ends of beam and carrying n intermediate point masses is presented in Figure 1. The total number of stations is $M^{'} = h + n$ from Figure 1. The kinds of coordinates which are used in this study are given below:

$x_{v^{'}}$ are the position vectors for the stations, $\left(1 \le v^{'} \le M'\right)$,

x_{p}^{*} are the position vectors of the intermediate point masses, $\left(1 \le p \le n\right)$,

$\overline{x}_{r}$ are the position vectors of the pinned supports, $\left(1 \le r \le h\right)$.

From Figure 1, the symbols of $1^{'}, 2^{'}, \ldots, v^{'}, \ldots, M^{'}-1, M^{'}$ above the x-axis refer to the numbering of stations. The symbols of $1, 2, \ldots, p, \ldots, n$ below the x-axis refer to the numbering of the intermediate point masses. The symbols of $(1),(2), \ldots,(r), \ldots,(h)$ below the x-axis refer to the numbering of the pinned supports.

Using Hamilton's principle, the equations of motion for axial-loaded Timoshenko beam can be written as:

$$\mathrm{EI}_{x} \cdot \frac{\partial^{2}\phi(x,t)}{\partial x^{2}} + \frac{AG}{\overline{k}} \cdot \left(\frac{\partial y(x,t)}{\partial x} - \phi(x,t)\right) - \frac{m \cdot I_{x}}{A} \cdot \frac{\partial^{2}\phi(x,t)}{\partial t^{2}} = 0 \tag{1.a}$$

$$\frac{AG \cdot}{\overline{k}} \cdot \left(\frac{\partial^{2} y(x,t)}{\partial x^{2}} - \frac{\partial \phi(x,t)}{\partial x}\right) - N \cdot \frac{\partial^{2} y(x,t)}{\partial x^{2}} - m \cdot \frac{\partial^{2} y(x,t)}{\partial t^{2}} = 0 \qquad \left(0 \le x \le L\right) \tag{1.b}$$

where $y(x,t)$ represents transverse deflection of the beam; $\phi(x,t)$ is the rotation angle due to bending moment; m is mass per unit length of the beam; N is the axial compressive force; A is the cross-section area; I_x is moment of inertia; $\overline{k}$ is the shape factor due to cross-section geometry of the beam; *E*, *G* is Young's modulus and shear modulus of the beam, respectively; *x* is the beam position; *t* is time variable.

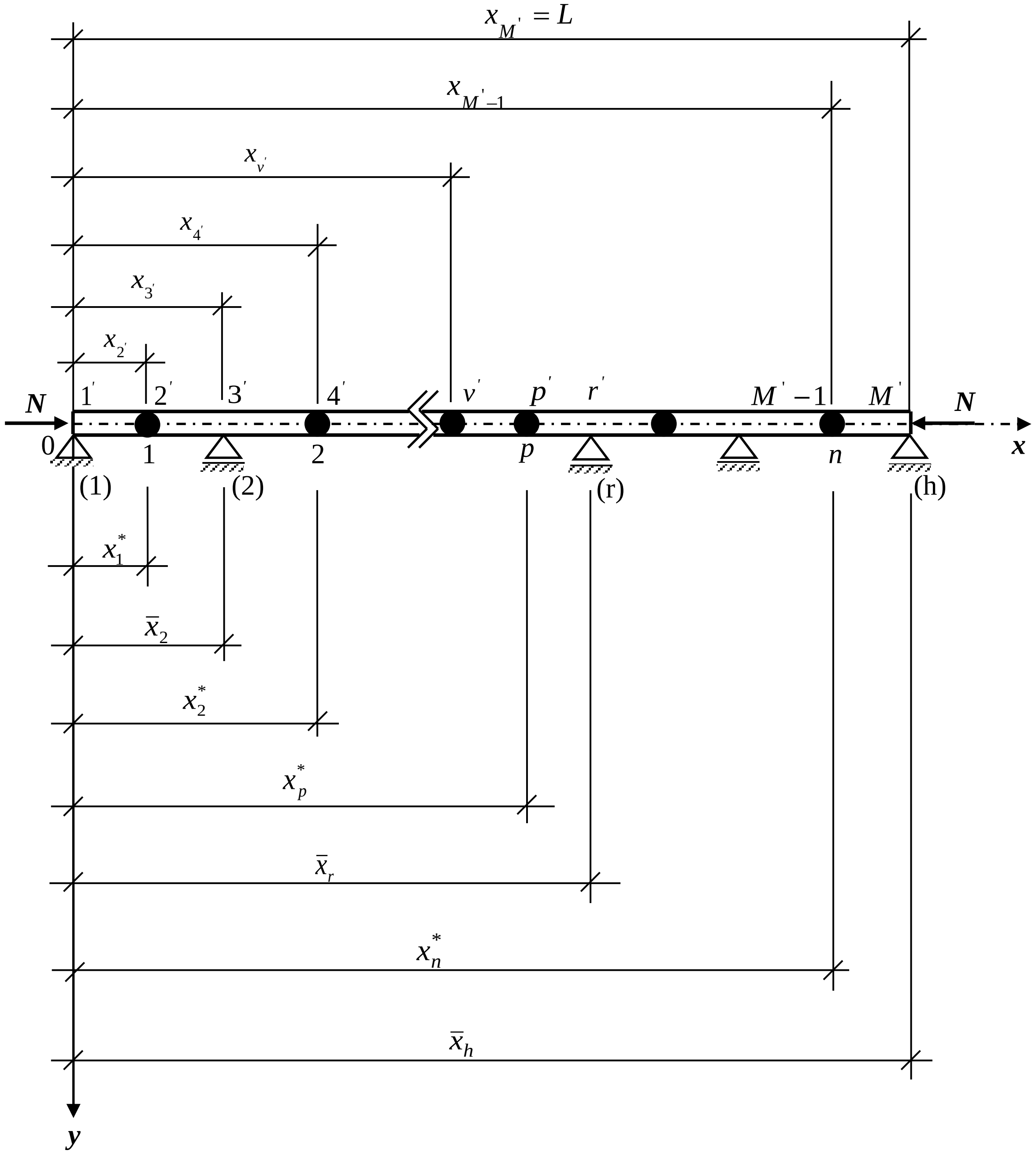

Figure 1. A Timoshenko uniform beam supported by *h* pins and carrying *n* intermediate point masses

The parameters appearing in the foregoing expressions have the following relationships:

$$\frac{\partial y(x,t)}{\partial x} = \phi(x,t) + \gamma(x,t) \tag{2.a}$$

$$M(x,t) = EI_x \cdot \frac{\partial \phi(x,t)}{\partial x} \tag{2.b}$$

$$T(x,t)=\frac{AG}{\bar{k}}\cdot\gamma(x,t)=\frac{AG}{\bar{k}}\cdot\left(\frac{\partial y(x,t)}{\partial x}-\phi(x,t)\right) \tag{2.c}$$

where $M(x,t)$ and $T(x,t)$ are the bending moment function and shear force function, respectively, and $\gamma(x,t)$ is the associated shearing deformation.

After some manipulations by using Eqs.(1) and (2), one obtains the following uncoupled equations of motion for the axial-loaded Timoshenko beam as:

$$\left(1-\frac{N\cdot\bar{k}}{AG}\right)\cdot EI_x\cdot\frac{\partial^4 y(x,t)}{\partial x^4}+N\cdot\frac{\partial^2 y(x,t)}{\partial x^2}+m\cdot\frac{\partial^2 y(x,t)}{\partial t^2}-\left(1+\frac{E\cdot\bar{k}}{G}-\frac{N\cdot\bar{k}}{AG}\right)\cdot\frac{\partial^4 y(x,t)}{\partial x^2\cdot\partial t^2}+\frac{m^2\cdot I_x\cdot\bar{k}}{A^2\cdot G}\cdot\frac{\partial^4 y(x,t)}{\partial t^4}=0 \tag{3.a}$$

$$\left(1-\frac{N\cdot\bar{k}}{AG}\right)\cdot EI_x\cdot\frac{\partial^4 \phi(x,t)}{\partial x^4}+N\cdot\frac{\partial^2 \phi(x,t)}{\partial x^2}+m\cdot\frac{\partial^2 \phi(x,t)}{\partial t^2}-\left(1+\frac{E\cdot\bar{k}}{G}-\frac{N\cdot\bar{k}}{AG}\right)\cdot\frac{\partial^4 \phi(x,t)}{\partial x^2\cdot\partial t^2}+\frac{m^2\cdot I_x\cdot\bar{k}}{A^2\cdot G}\cdot\frac{\partial^4 \phi(x,t)}{\partial t^4}=0 \tag{3.b}$$

The general solution of Eq.(3) can be obtained by using the method of separation of variables as:

$$y(z,t)=y(z)\cdot\sin(\omega\cdot t) \tag{4.a}$$

$$\phi(x,t)=\phi(x)\cdot\sin(\omega\cdot t) \qquad (0\le z\le 1) \tag{4.b}$$

in which

$$y(z)=\left[C_1.\cosh(D_1.z)+C_2.\sinh(D_1.z)+C_3.\cos(D_2.z)+C_4.\sin(D_2.z)\right];$$

$$\phi(z)=\left[K_3\cdot C_1.\sinh(D_1.z)+K_3\cdot C_2.\cosh(D_1.z)+K_4\cdot C_3.\sin(D_2.z)-K_4\cdot C_4.\cos(D_2.z)\right];$$

$$D_1=\sqrt{\frac{1}{2}\cdot\left(-\beta+\sqrt{\beta^2+4\cdot\alpha^4}\right)};\ D_2=\sqrt{\frac{1}{2}\cdot\left(\beta+\sqrt{\beta^2+4\cdot\alpha^4}\right)};$$

$$\beta=\frac{\left[\frac{N_r\cdot\pi^2\cdot EI_x}{L^2}+\left(1+\frac{E\cdot\bar{k}}{AG}-\frac{N_r\cdot\pi^2\cdot EI_x\cdot\bar{k}}{AG\cdot L^2}\right)\cdot\frac{m\cdot I_x}{A}\cdot\omega^2\right]\cdot L^2}{\left(1-\frac{N_r\cdot\pi^2\cdot EI_x\cdot\bar{k}}{AG\cdot L^2}\right)\cdot EI_x};$$

$$\alpha^4 = \frac{\lambda^4 \cdot EI_x - \dfrac{m^2 \cdot I_x \cdot \bar{k} \cdot \omega^4 \cdot L^4}{A^2 \cdot G}}{\left(1 - \dfrac{N_r \cdot \pi^2 \cdot EI_x \cdot \bar{k}}{AG \cdot L^2}\right) \cdot EI_x}; \qquad N_r = \frac{N \cdot L^2}{\pi^2 \cdot EI_x}$$ (nondimensionalized multiplication factor for the axial compressive force) ; $\lambda = \sqrt[4]{\dfrac{m.\omega^2.L^4}{EI_x}}$ (frequency factor)

$$K_3 = \frac{AG \cdot D_1}{\bar{k} \cdot \left(-EI_x \cdot D_1^2 - \dfrac{m \cdot I_x}{A} \cdot \omega^2 + \dfrac{AG}{\bar{k}}\right)}; \quad K_4 = \frac{-AG \cdot D_2}{\bar{k} \cdot \left(EI_x \cdot D_2^2 - \dfrac{m \cdot I_x}{A} \cdot \omega^2 + \dfrac{AG}{\bar{k}}\right)};$$

$z = \dfrac{x}{L}$; C_1, ..., C_4 are the constants of integration; L is the total length of the beam; ω is the natural circular frequency of the vibrating system.

The bending moment and shear force functions of the beam with respect to z are given below:

$$M(z,t) = \frac{EI_x}{L} \cdot \frac{d\phi(z)}{dz} \cdot \sin(\omega \cdot t) \tag{5.a}$$

$$T(z,t) = \frac{AG}{\bar{k}} \cdot \left(\frac{1}{L} \cdot \frac{dy(z)}{dz} - \phi(z)\right) \cdot \sin(\omega \cdot t) \tag{5.b}$$

3. DETERMINATION OF NATURAL FREQUENCIES AND MODE SHAPES

The position is written due to the values of the displacement, slope, bending moment and shear force functions at the locations of z and t for Timoshenko beam, as:

$$\{S(z,t)\}^T = \{y(z) \quad \phi(z) \quad M(z) \quad T(z)\} \cdot \sin(\omega.t) \tag{6}$$

where $\{S(z,t)\}$ shows the position vector.

The boundary conditions for the left-end support of the beam are written as:

$$y_{1'}(z=0) = 0 \tag{7.a}$$

$$M_{1'}(z=0) = 0 \tag{7.b}$$

From Eqs.(4.a) and (5.a), the boundary conditions for the left-end support can be written in matrix equation form as:

$$[B_{1'}] \cdot \{C_{1'}\} = \{0\} \tag{8.a}$$

$$\begin{array}{cccc c} 1 & 2 & 3 & 4 & \\ \end{array}$$

$$\begin{array}{c} \begin{bmatrix} 1 & 0 & 1 & 0 \\ K_1 & 0 & -K_2 & 0 \end{bmatrix} \end{array} \begin{array}{c} 1 \\ 2 \end{array} \cdot \begin{Bmatrix} C_{1',1} \\ C_{1',2} \\ C_{1',3} \\ C_{1',4} \end{Bmatrix} = \begin{Bmatrix} 0 \\ 0 \end{Bmatrix} \tag{8.b}$$

where $K_1 = \dfrac{EI_x \cdot K_3 \cdot D_1}{L}$; $K_2 = -\dfrac{EI_x \cdot K_4 \cdot D_2}{L}$

The boundary conditions for the p^{th} intermediate point mass are written by using continuity of deformations, slopes and equilibrium of bending moments and shear forces, as (the station numbering corresponding to the p^{th} intermediate point mass is represented by p'):

$$y^L_{p'}(z_{p'}) = y^R_{p'}(z_{p'}) \tag{9.a}$$

$$\phi^L_{p'}(z_{p'}) = \phi^R_{p'}(z_{p'}) \tag{9.b}$$

$$M^L_{p'}(z_{p'}) = M^R_{p'}(z_{p'}) \tag{9.c}$$

$$T^L_{p'}(z_{p'}) + m_p \cdot \omega^2 \cdot y^L_{p'}(z_{p'}) = T^R_{p'}(z_{p'}) \tag{9.d}$$

where m_p is the magnitude of the p^{th} intermediate point mass; L and R refer to the left side and right side of the p^{th} intermediate point mass, respectively.

In Appendix, the boundary conditions for the p^{th} intermediate point mass are presented in matrix equation form.

The boundary conditions for the r^{th} support are written by using continuity of deformations, slopes and equilibrium of bending moments, as (the station numbering corresponding to the r^{th} intermediate support is represented by r'):

$$y^L_{r'}(z_{r'}) = y^R_{r'}(z_{r'}) = 0 \tag{10.a}$$

$$\phi^L_{r'}(z_{r'}) = \phi^R_{r'}(z_{r'}) \tag{10.b}$$

$$M^L_{r'}(z_{r'}) = M^R_{r'}(z_{r'}) \tag{10.c}$$

In Appendix, the boundary conditions for the r^{th} intermediate support are presented in matrix equation.

The boundary conditions for the right-end support of the beam are written as:

$$y_{M'}(z=1)=0 \tag{11.a}$$

$$M_{M'}(z=1)=0 \tag{11.b}$$

From Eqs.(4.a) and (5.a), the boundary conditions for the right-end support can be written in matrix equation form as:

$$\left[B_{M'}\right]\cdot\left\{C_{M'}\right\}=\{0\} \tag{12.a}$$

$$\begin{array}{cccc} 4M_i'+1 & 4M_i'+2 & 4M_i'+3 & 4M_i'+4 \end{array}$$
$$\left[\begin{array}{cccc} \cosh(D_1) & \sinh(D_1) & \cos(D_2) & \sin(D_2) \\ K_1\cdot\cosh(D_1) & K_1\cdot\sinh(D_1) & -K_2\cdot\cos(D_2) & -K_2\cdot\sin(D_2) \end{array}\right]\begin{array}{c} q-1 \\ q \end{array}\cdot\begin{Bmatrix} C_{M',1} \\ C_{M',2} \\ C_{M',3} \\ C_{M',4} \end{Bmatrix}=\begin{Bmatrix} 0 \\ 0 \end{Bmatrix} \tag{12.b}$$

where M_i' is the total number of intermediate stations and is given by:

$$M_i'=M'-2 \tag{13.a}$$

with

$$M'=h+n \tag{13.b}$$

In Eq.(13.b), M' is the total number of stations.

In Eq.(12.b), q denotes the total number of equations for integration constants given by

$$q=2+4\cdot\left(M'-2\right)+2 \tag{14}$$

From Eq.(14), it can be seen that; the left-end support of the beam has two equations, each intermediate station of the beam has four equations and the right-end support of the beam has two equations.

In this paper, the coefficient matrices for left-end support, each intermediate point mass, each intermediate pinned support and right-end support of a Timoshenko beam are derived, respectively. In the next step, the NAT is used to establish the overall coefficient matrix for the whole vibrating system as is given in Eq.(15). In the last step, for non-trivial solution, equating the last overall coefficient matrix to zero one determines the natural frequencies of the vibrating system as is given in Eq.(16) and substituting the last integration constants into the related eigenfunctions one determines the associated mode shapes.

$$[B]\cdot\{C\}=\{0\} \tag{15}$$

$$|B| = 0 \tag{16}$$

4. THE DIFFERENTIAL TRANSFORM METHOD (DTM)

Partial differential equations are often used to describe engineering problems whose closed form solutions are very difficult to establish in many cases. Therefore, approximate numerical methods are often preferred. However, in spite of the advantages of these on hand methods and the computer codes that are based on them, closed form solutions are more attractive due to their implementation of the physics of the problem and their convenience for parametric studies. Moreover, closed form solutions have the capability and facility to solve inverse problems of determining and designing the geometry and characteristics of an engineering system and to achieve a prescribed behavior of the system. Considering the advantages of the closed form solutions mentioned above, DTM is introduced in this study as the solution method.

DTM is a semi-analytic transformation technique based on Taylor series expansion and is a useful tool to obtain analytical solutions of the differential equations. Certain transformation rules are applied and the governing differential equations and the boundary conditions of the system are transformed into a set of algebraic equations in terms of the differential transforms of the original functions in DTM. The solution of these algebraic equations gives the desired solution of the problem. The difference from high-order Taylor series method is that; Taylor series method requires symbolic computation of the necessary derivatives of the data functions and is expensive for large orders. DTM is an iterative procedure to obtain analytic Taylor series solutions of differential equations.

A function $y(z)$, which is analytic in a domain *D*, can be represented by a power series with a center at $z = z_0$, any point in *D*. The differential transform of the function $y(z)$ is given by

$$Y(k) = \frac{1}{k!} \cdot \left(\frac{d^k y(z)}{dz^k} \right)_{z=z_0} \tag{17}$$

where $y(z)$ is the original function and $Y(k)$ is the transformed function. The inverse transformation is defined as:

$$y(z) = \sum_{k=0}^{\infty} (z - z_0)^k \cdot Y(k) \tag{18}$$

From Eqs.(17) and (18) we get

$$y(z) = \sum_{k=0}^{\infty} \frac{(z - z_0)^k}{k!} \cdot \left(\frac{d^k y(z)}{dz^k} \right)_{z=z_0} \tag{19}$$

Eq.(19) implies that the concept of the differential transformation is derived from Taylor's series expansion, but the method does not evaluate the derivatives symbolically. However, relative derivatives are calculated by iterative procedure that are described by the transformed equations of the original functions. In real applications, the function $y(z)$ in Eq.(18) is expressed by a finite series and can be written as:

$$y(z)=\sum_{k=0}^{\bar{N}}(z-z_0)^k\cdot Y(k) \tag{20}$$

Eq.(20) implies that $\sum_{k=\bar{N}+1}^{\infty}(z-z_0)^k\,Y(k)$ is negligibly small. Where $\bar{N}$ is series size and the value of $\bar{N}$ depends on the convergence of the eigenvalues.

Theorems that are frequently used in differential transformation of the differential equations and the boundary conditions are introduced in Table 1 and Table 2, respectively.

Table 1. DTM theorems used for equations of motion

Original Function	Transformed Function
$y(z)=u(z)\pm v(z)$	$Y(k)=U(k)\pm V(k)$
$y(z)=a\cdot u(z)$	$Y(k)=a\cdot U(k)$
$y(z)=\dfrac{d^m u(z)}{dz^m}$	$Y(k)=\dfrac{(k+m)!}{k!}\cdot U(k+m)$
$y(z)=u(z)\cdot v(z)$	$Y(k)=\sum_{r=0}^{k}U(r)\cdot V(k-r)$

Table 2. DTM theorems used for boundary conditions

$z = 0$		$z = 1$	
Original Boundary Conditions	Transformed Boundary Conditions	Original Boundary Conditions	Transformed Boundary Conditions
$y(0)=0$	$Y(0)=0$	$y(1)=0$	$\sum_{k=0}^{\infty}Y(k)=0$
$\dfrac{dy}{dz}(0)=0$	$Y(1)=0$	$\dfrac{dy}{dz}(1)=0$	$\sum_{k=0}^{\infty}k\cdot Y(k)=0$
$\dfrac{d^2y}{dz^2}(0)=0$	$Y(2)=0$	$\dfrac{d^2y}{dz^2}(1)=0$	$\sum_{k=0}^{\infty}k\cdot(k-1)\cdot Y(k)=0$
$\dfrac{d^3y}{dz^3}(0)=0$	$Y(3)=0$	$\dfrac{d^3y}{dz^3}(1)=0$	$\sum_{k=0}^{\infty}k\cdot(k-1)\cdot(k-2)\cdot Y(k)=0$

4.1. Using Differential Transformation o Solve Motion Equations

Eqs.(1.a) and (1.b) can be rewritten by using the method of separation of variables as follows:

$$\frac{d^2\phi(z)}{dz^2} = -\left(\frac{AG \cdot L}{EI_x \cdot \bar{k}}\right) \cdot \frac{dy(z)}{dz} + \left(\frac{AG \cdot L^2}{EI_x \cdot \bar{k}} - \frac{\lambda^4 \cdot I_x}{A \cdot L^2}\right) \cdot \phi(z) \tag{21.a}$$

$$\frac{d^2y(z)}{dz^2} = \left(\frac{AG \cdot L^3}{AG \cdot L^2 - N_r \cdot \pi^2 \cdot EI_x \cdot \bar{k}}\right) \cdot \frac{d\phi(z)}{dz} - \left(\frac{\lambda^4 \cdot EI_x \cdot \bar{k}}{AG \cdot L^2 - N_r \cdot \pi^2 \cdot EI_x \cdot \bar{k}}\right) \cdot y(z)$$
$$(0 \le z \le 1) \tag{21.b}$$

The differential transform method is applied to Eqs.(21.a) and (21.b) by using the theorems introduced in Table 1 and the following expression are obtained:

$$\Phi(k+2) = -\frac{1}{(k+2)} \cdot \left(\frac{AG \cdot L}{EI_x \cdot \bar{k}}\right) \cdot Y(k+1) + \frac{1}{(k+1) \cdot (k+2)} \cdot \left(\frac{AG \cdot L^2}{EI_x \cdot \bar{k}} - \frac{\lambda^4 \cdot I_x}{A \cdot L^2}\right) \cdot \Phi(k) \tag{22.a}$$

$$Y(k+2) = \frac{1}{(k+2)} \cdot \left(\frac{AG \cdot L^3}{AG \cdot L^2 - N_r \cdot \pi^2 \cdot EI_x \cdot \bar{k}}\right) \cdot \Phi_i(k+1)$$
$$- \frac{1}{(k+1) \cdot (k+2)} \cdot \left(\frac{\lambda^4 \cdot EI_x \cdot \bar{k}}{AG \cdot L^2 - N_r \cdot \pi^2 \cdot EI_x \cdot \bar{k}}\right) \cdot Y(k) \tag{22.b}$$

where $Y(k)$ and $\Phi(k)$ are the transformed functions of $y(z)$ and $\phi(z)$, respectively.

The differential transform method is applied to Eqs.(5.a) and (5.b) by using the theorems introduced in Table 1 and the following expression are obtained:

$$\overline{M}(k) = (k+1) \cdot \left(\frac{EI_x}{L}\right) \cdot \Phi(k+1) \tag{23.a}$$

$$\overline{T}(k) = \frac{AG}{\bar{k}} \cdot \left(\frac{k+1}{L} \cdot Y(k+1) - \Phi(k)\right) \tag{23.b}$$

where $\overline{M}(k)$ and $\overline{T}(k)$ are the transformed functions of $M(z)$ and $T(z)$, respectively.

Applying DTM to Eqs.(7.a) and (7.b), the transformed boundary conditions for the left-end support are written as:

$$Y_{1'}(0) = \Phi_{1'}(1) = 0 \tag{24}$$

The boundary conditions and the transformed boundary conditions of the p^{th} intermediate point mass and the r^{th} intermediate support by applying the differential transform method, using the theorems introduced in Table 2 are presented in Table 3.

Applying DTM to Eqs.(11.a) and (11.b), the transformed boundary conditions for the right-end support are written as:

$$\sum_{k=0}^{\bar{N}} Y_{M'}(k) = 0 \tag{25.a}$$

$$\sum_{k=0}^{\bar{N}} \overline{M}_{M'}(k) = 0 \tag{25.b}$$

Substituting the boundary conditions expressed in Eqs.(24) and (25) into Eq.(22) and taking $Y_{1'}(1) = c_1$, $\Phi_{1'}(0) = c_2$; the following matrix expression is obtained:

$$\begin{bmatrix} A_{11}^{(\bar{N})}(\omega) & A_{12}^{(\bar{N})}(\omega) \\ A_{21}^{(\bar{N})}(\omega) & A_{22}^{(\bar{N})}(\omega) \end{bmatrix} \cdot \begin{Bmatrix} c_1 \\ c_2 \end{Bmatrix} = \begin{Bmatrix} 0 \\ 0 \end{Bmatrix} \tag{26}$$

where c_1 and c_2 are constants and $A_{a1}^{(\bar{N})}(\omega)$, $A_{a2}^{(\bar{N})}(\omega)$ (a =1, 2) are polynomials of ω corresponding $\bar{N}$.

In the last step, for non-trivial solution, equating the coefficient matrix that is given in Eq.(26) to zero one determines the natural frequencies of the vibrating system as is given in Eq.(27).

$$\begin{vmatrix} A_{11}^{(\bar{N})}(\omega) & A_{12}^{(\bar{N})}(\omega) \\ A_{21}^{(\bar{N})}(\omega) & A_{22}^{(\bar{N})}(\omega) \end{vmatrix} = 0 \tag{27}$$

The j^{th} estimated eigenvalue, $\omega_j^{(\bar{N})}$ corresponds to $\bar{N}$ and the value of $\bar{N}$ is determined as:

$$\left| \omega_j^{(\bar{N})} - \omega_j^{(\bar{N}-1)} \right| \le \varepsilon \tag{28}$$

where $\omega_j^{(\bar{N}-1)}$ is the j^{th} estimated eigenvalue corresponding to $\left(\bar{N}-1\right)$ and ε is the small tolerance parameter. If Eq.(28) is satisfied, the j^{th} estimated eigenvalue, $\omega_j^{(\bar{N})}$ is obtained.

Table 3. The boundary conditions and the transformed boundary conditions of the p^{th} intermediate point mass and the r^{th} intermediate support

Boundary Conditions	Transformed Boundary Conditions
$y_{p'}^{L}\left(z_{p'}\right)=y_{p'}^{R}\left(z_{p'}\right)$	$\sum_{k=0}^{\bar{N}} z_{p'}^{k}\cdot Y_{p'}^{L}(k)-\sum_{k=0}^{\bar{N}} z_{p'}^{k}\cdot Y_{p'}^{R}(k)=0$
$\phi_{p'}^{L}\left(z_{p'}\right)=\phi_{p'}^{R}\left(z_{p'}\right)$	$\sum_{k=0}^{\bar{N}} z_{p'}^{k}\cdot \Phi_{p'}^{L}(k)-\sum_{k=0}^{\bar{N}} z_{p'}^{k}\cdot \Phi_{p'}^{R}(k)=0$
$M_{p'}^{L}\left(z_{p'}\right)=M_{p'}^{R}\left(z_{p'}\right)$	$\sum_{k=0}^{\bar{N}} z_{p'}^{k}\cdot \overline{M}_{p'}^{L}(k)-\sum_{k=0}^{\bar{N}} z_{p'}^{k}\cdot \overline{M}_{p'}^{R}(k)=0$
$T_{p'}^{L}\left(z_{p'}\right)+m_p\cdot\omega^2\cdot y_{p'}^{L}\left(z_{p'}\right)=T_{p'}^{R}\left(z_{p'}\right)$	$\sum_{k=0}^{\bar{N}} z_{p'}^{k}\cdot \overline{T}_{p'}^{L}(k)+m_p\cdot\omega^2\cdot\sum_{k=0}^{\bar{N}} z_{p'}^{k}\cdot Y_{p'}^{L}(k)-\sum_{k=0}^{\bar{N}} z_{p'}^{k}\cdot \overline{T}_{p'}^{R}(k)=0$
$y_{r'}^{L}\left(z_{r'}\right)=y_{r'}^{R}\left(z_{r'}\right)=0$	$\sum_{k=0}^{\bar{N}} z_{r'}^{k}\cdot Y_{r'}^{L}(k)=\sum_{k=0}^{\bar{N}} z_{r'}^{k}\cdot Y_{r'}^{R}(k)=0$
$\phi_{r'}^{L}\left(z_{r'}\right)=\phi_{r'}^{R}\left(z_{r'}\right)$	$\sum_{k=0}^{\bar{N}} z_{r'}^{k}\cdot \Phi_{r'}^{L}(k)-\sum_{k=0}^{\bar{N}} z_{r'}^{k}\cdot \Phi_{r'}^{R}(k)=0$
$M_{r'}^{L}\left(z_{r'}\right)=M_{r'}^{R}\left(z_{r'}\right)$	$\sum_{k=0}^{\bar{N}} z_{r'}^{k}\cdot \overline{M}_{r'}^{L}(k)-\sum_{k=0}^{\bar{N}} z_{r'}^{k}\cdot \overline{M}_{r'}^{R}(k)=0$

The procedure that is explained below can be used to plot the mode shapes of Timoshenko multi-span beam carrying multiple point masses. The following equalities can be written by using Eq.(26):

$$A_{11}(\omega)\cdot c_1+A_{12}(\omega)\cdot c_2=0 \tag{29}$$

Using Eq. (29), the constant c_2 can be obtained in terms of c_1 as follows:

$$c_2=-\frac{A_{11}(\omega)}{A_{12}(\omega)}\cdot c_1 \tag{30}$$

All transformed functions can be expressed in terms of ω, c_1 and c_2. Since c_2 has been written in terms of c_1 above, $Y(k)$, $\Phi(k)$, $\overline{M}(k)$ and $\overline{T}(k)$ can be expressed in terms c_1 as follows:

$$Y(k)=Y(\omega,c_1) \tag{31}$$

$$\Phi(\mathrm{k}) = \Phi(\omega, \mathrm{c}_1) \tag{32}$$

$$\overline{\mathrm{M}}(\mathrm{k}) = \overline{\mathrm{M}}(\omega, \mathrm{c}_1) \tag{33}$$

$$\overline{\mathrm{T}}(\mathrm{k}) = \overline{\mathrm{T}}(\omega, \mathrm{c}_1) \tag{34}$$

The mode shapes can be plotted for several values of ω by using Eq.(31).

5. NUMERICAL ANALYSIS AND DISCUSSIONS

In this study, three numerical examples are considered. For three numerical examples, natural frequencies of the beam, ω_i (i = 1, …, 5) are calculated by using a computer program developed as part of the research undertaken in this paper. In this program, the secant method is used in which determinant values are evaluated for a range (ω_i) values. The (ω_i) value causing a sign change between the successive determinant values is a root of frequency equation and means a frequency for the system.

Natural frequencies are found by determining values for which the determinant of the coefficient matrix is equal to zero. There are various methods for calculating the roots of the frequency equation. One common used and simple technique is the secant method in which a linear interpolation is employed. The eigenvalues, the natural frequencies, are determined by a trial and error method based on interpolation and the bisection approach. One such procedure consists of evaluating the determinant for a range of frequency values, ω_i. When there is a change of sign between successive evaluations, there must be a root lying in this interval. The iterative computations are determined when the value of the determinant changed sign due to a change of 10^{-4} in the value of ω_i.

All numerical results of this paper are obtained based on a uniform, circular Timoshenko beam with the following data as:

Diameter d =0.05 m ; $EI_x = 6.34761 \times 10^4$ Nm^2 ; m =15.3875 kg/m ; L =1.0 m ; for the shear effect, $\bar{k} = 4/3$ and $AG = 1.562489231 \times 10^8$ N; for the axial force effect, N_r = 0, 0.25, 0.50 and 0.75.

5.1. Free Vibration Analysis of the Uniform Pinned-Pinned Timoshenko Beam Carrying Three to Five Intermediate Point Masses

In the first numerical example (see Figure 2 and Figure 3), the uniform pinned-pinned Timoshenko beam carrying three to five intermediate point masses is considered. In this numerical example, for the case with three intermediate point masses, the magnitudes and locations of the intermediate point masses are taken as: $m_1 = (0.20 \cdot m \cdot L)$, $m_2 = (0.50 \cdot m \cdot L)$ and $m_3 = (1.00 \cdot m \cdot L)$ located at $z_1^* = 0.10$, $z_2^* = 0.50$ and $z_3^* = 0.90$, respectively. For the case with five intermediate point masses, the magnitudes and locations of the intermediate point masses are taken as: $m_1 = (0.20 \cdot m \cdot L)$, $m_2 = (0.30 \cdot m \cdot L)$, $m_3 = (0.50 \cdot m \cdot L)$,

$m_4 = (0.65 \cdot m \cdot L)$ and $m_5 = (1.00 \cdot m \cdot L)$ located at $z_1^* = 0.10$, $z_2^* = 0.30$, $z_3^* = 0.50$, $z_4^* = 0.70$ and $z_5^* = 0.90$, respectively.

Using DTM, the frequency values obtained for the first five modes are presented in Table 4 being compared with the frequency values obtained by using NAT for N_r = 0, 0.25, 0.50, and 0.75 and for N_r = 0.75, mode shapes for the model with five intermediate point masses of the pinned-pinned Timoshenko beam are presented in Figure 4.

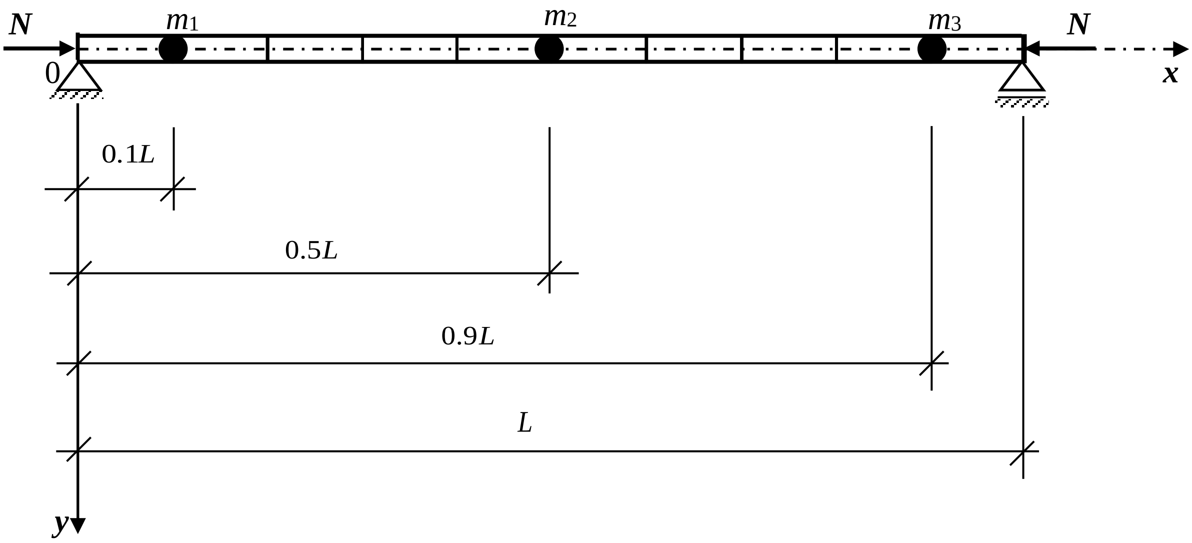

Figure 2. A pinned-pinned Timoshenko beam carrying three intermediate point masses

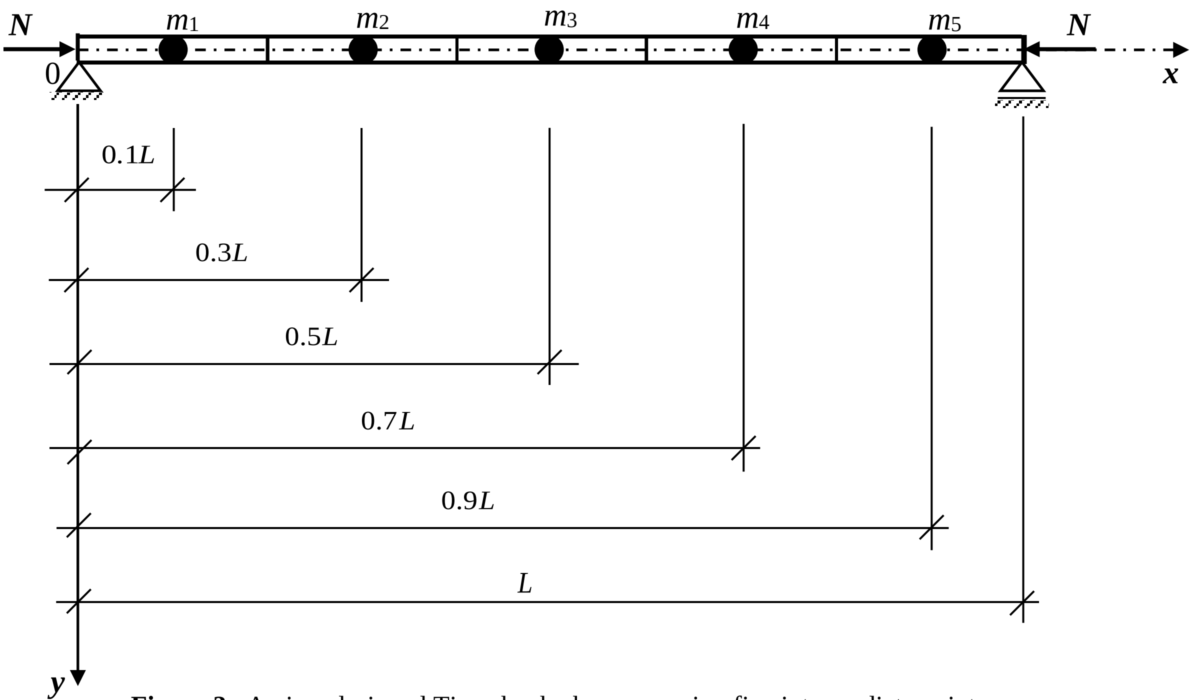

Figure 3. A pinned-pinned Timoshenko beam carrying five intermediate point masses

From Table 4 one can sees that increasing N_r causes a decrease in the first five mode frequency values for two cases, as expected. Similarly, as the number of the intermediate point masses is increased for N_r is being constant, the first five frequency values are decreased.

In application od DTM, the natural frequency values of the beams are calculated by in increasing series size $\overline{N}$. In Table 4, convergences of the first five natural frequencies are introduced. Here, it is seen that; for the case with three intermediate point masses, when the series size is taken 54; for the case with five intermediate point masses, when the series size is taken 60, the natural frequency values of the fifth mode can be appeared. Additionally, here it is seen that higher modes appear when more terms are taken into account in DTM applications. Thus, depending on the order of the required mode, one must try a few values for the term number at the beginning of the calculations in order to find the adequate number of terms.

Table 4. The first five natural frequencies of the uniform pinned-pinned Timoshenko beam carrying multiple intermediate point masses for different values of N_r

No. of point masses, *n*	ω_α (rad/sec)	METHOD	$N_r = 0.00$	$N_r = 0.25$	$N_r = 0.50$	$N_r = 0.75$
3	ω_1	DTM $(\overline{N} = 34)$	422.7835	366.2711	299.1718	211.6306
		NAT	422.7835	366.2710	299.1709	211.6298
	ω_2	DTM $(\overline{N} = 42)$	1766.4628	1715.5836	1662.5698	1607.1784
		NAT	1766.4630	1715.5833	1662.5692	1607.1789
	ω_3	DTM $(\overline{N} = 48)$	3181.5224	3131.6510	3081.1469	3029.9900
		NAT	3181.5220	3131.6503	3081.1458	3029.9894
	ω_4	DTM $(\overline{N} = 50)$	6721.0894	6664.8292	6608.0762	6550.8178
		NAT	6721.0894	6664.8291	6608.0757	6550.8171
	ω_5	DTM $(\overline{N} = 54)$	9674.2838	9623.4595	9572.3528	9520.9459
		NAT	9674.2835	9623.4595	9572.3528	9520.9457
5	ω_1	DTM $(\overline{N} = 36)$	338.5581	293.3282	239.6171	169.5258
		NAT	338.5581	293.3282	239.6171	169.5258
	ω_2	DTM $(\overline{N} = 44)$	1355.4886	1312.7533	1268.5024	1222.5708
		NAT	1355.4885	1312.7530	1268.5019	1222.5698
	ω_3	DTM $(\overline{N} = 52)$	2893.3531	2854.1318	2814.2714	2773.7424
		NAT	2893.3528	2854.1313	2814.2702	2773.7415
	ω_4	DTM $(\overline{N} = 56)$	4530.3380	4498.4436	4466.2835	4433.8462
		NAT	4530.3380	4498.4436	4466.2835	4433.8460
	ω_5	DTM $(\overline{N} = 60)$	7109.2305	7068.1216	7026.7792	6985.2004
		NAT	7109.2305	7068.1215	7026.7789	6985.1995

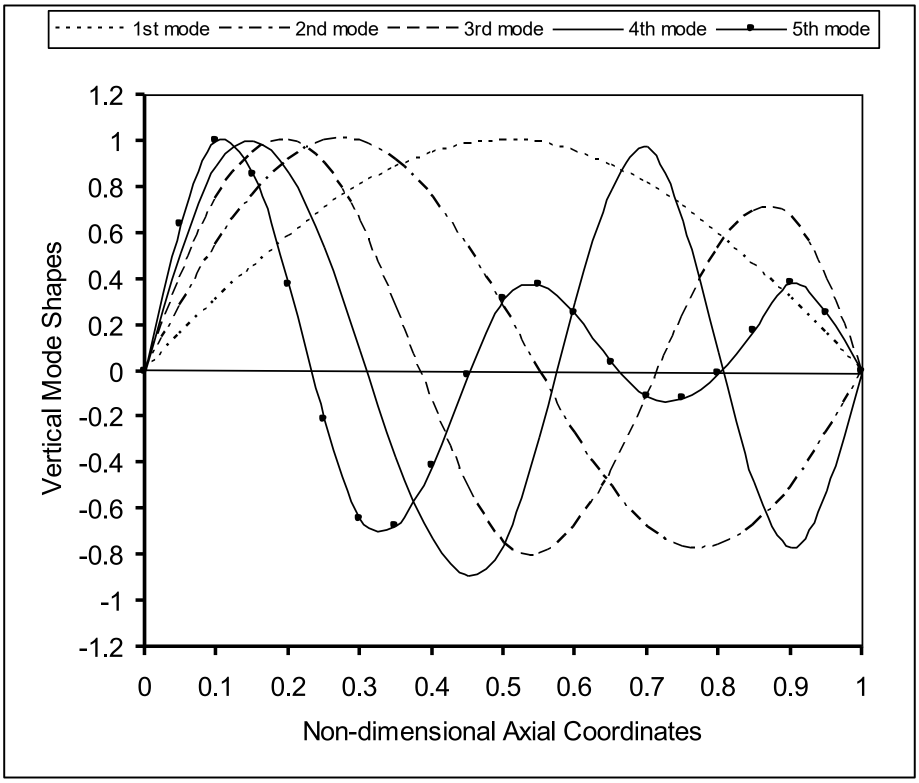

Figure 4. The first five mode shapes for the model with five intermediate point masses of the pinned-pinned Timoshenko beam, N_r = 0.75

5.2. Free Vibration Analysis of the Uniform Two-Span Timoshenko Beam Carrying One Intermediate Point Mass

In the second numerical example (see Figure 5), the uniform two-span Timoshenko beam carrying one intermediate point mass is considered. In this numerical example, the magnitude and location of the intermediate point mass are taken as: $m_1 = (0.50 \cdot m \cdot L)$ at $z_1^* = 0.50$ and the location of intermediate pinned support is at $\bar{z}_1 = 0.4$.

Using DTM, the frequency values obtained for the first five modes are presented in Table 5 being compared with the frequency values obtained by using NAT for N_r = 0, 0.25, 0.50, and 0.75 and for N_r = 0.75, mode shapes of the uniform two-span Timoshenko beam carrying one intermediate point mass are presented in Figure 6.

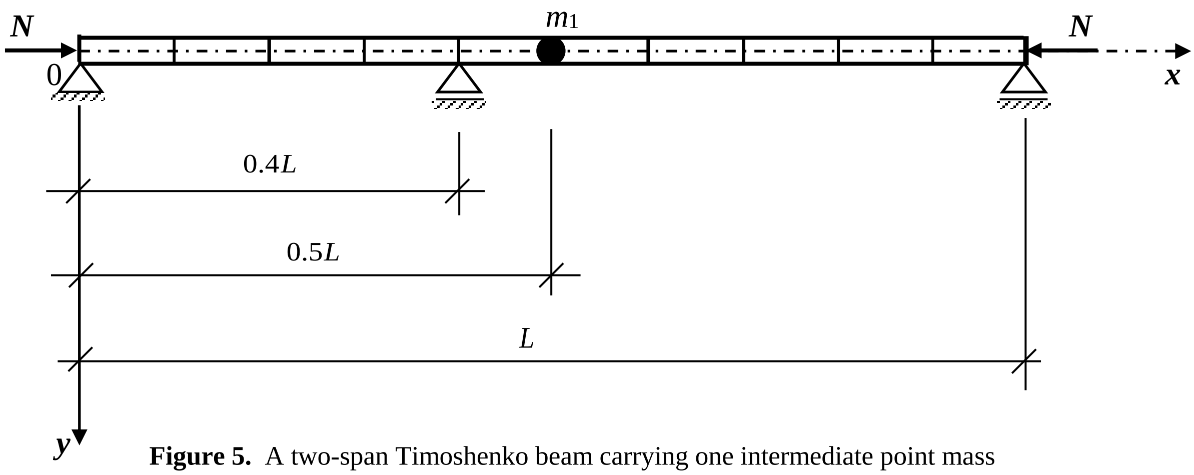

Figure 5. A two-span Timoshenko beam carrying one intermediate point mass

Table 5. The first five natural frequencies of the uniform pinned-pinned Timoshenko beam with an intermediate pinned support and carrying one intermediate point mass for different values of N_r

ω_α (rad/sec)	METHOD	$N_r = 0.00$	$N_r = 0.25$	$N_r = 0.50$	$N_r = 0.75$
ω_1	DTM $(\overline{N} = 38)$	1856.4217	1795.2700	1731.6620	1665.3084
	NAT	1856.4217	1795.2700	1731.6619	1665.3080
ω_2	DTM $(\overline{N} = 46)$	4487.7604	4423.8529	4358.9435	4292.9863
	NAT	4487.7600	4423.8524	4358.9428	4292.9854
ω_3	DTM $(\overline{N} = 52)$	6015.0752	5965.9946	5916.4760	5866.5076
	NAT	6015.0752	5965.9943	5916.4754	5866.5068
ω_4	DTM $(\overline{N} = 58)$	11901.1078	11837.0343	11772.6287	11707.8852
	NAT	11901.1078	11837.0342	11772.6281	11707.8845
ω_5	DTM $(\overline{N} = 62)$	16654.4519	16589.1244	16523.5457	16457.7137
	NAT	16654.4518	16589.1240	16523.5451	16457.7125

From Table 5 one can sees that, as the axial compressive force acting to the beam is increased, the first five natural frequency values are decreased. It can be seen from Figure 6 that, all five mode curves pass through the intermediate pinned support located at $\bar{z}_1 = 0.4$.

In application of DTM, the natural frequency values of the beams are calculated by increasing series size $\bar{N}$. In Table 5, convergences of the first five natural frequencies are introduced. Here, it is seen that; when the series size is taken 62, the natural frequency values of the fifth mode appears.

5.3. Free Vibration Analysis of the Uniform Multi-Span Timoshenko Beam Carrying Five Intermediate Point Masses

In the third numerical example (see Figure 7), the uniform Timoshenko beam carrying five intermediate point masses with one to four intermediate pinned supports is considered. In this numerical example, the magnitudes and locations of the intermediate point masses are taken as: $m_1 = (0.20 \cdot m \cdot L)$, $m_2 = (0.30 \cdot m \cdot L)$, $m_3 = (0.50 \cdot m \cdot L)$, $m_4 = (0.65 \cdot m \cdot L)$ and $m_5 = (1.00 \cdot m \cdot L)$ located at $z_1^* = 0.10$, $z_2^* = 0.30$, $z_3^* = 0.50$, $z_4^* = 0.70$ and $z_5^* = 0.90$, respectively. In this example, three cases of the intermediate pinned supports are considered.

For the case with one intermediate pinned support, the location of the intermediate pinned support is taken as $\bar{z}_1 = 0.4$.For the case with two intermediate pinned supports, the locations of the intermediate pinned supports are taken as $\bar{z}_1 = 0.4$ and $\bar{z}_2 = 0.6$, respectively. For the case with four intermediate pinned supports, the locations of the intermediate pinned supports are taken as $\bar{z}_1 = 0.2$, $\bar{z}_2 = 0.4$, $\bar{z}_3 = 0.6$ and $\bar{z}_4 = 0.8$, respectively.

Using DTM, the frequency values obtained for the first five modes are presented in Table 6 being compared with the frequency values obtained by using NAT for N_r = 0, 0.25, 0.50, and 0.75 and for N_r = 0.75, mode shapes of pinned-pinned Timoshenko beam carrying five intermediate point masses and with two intermediate pinned supports are presented in Figure 8.

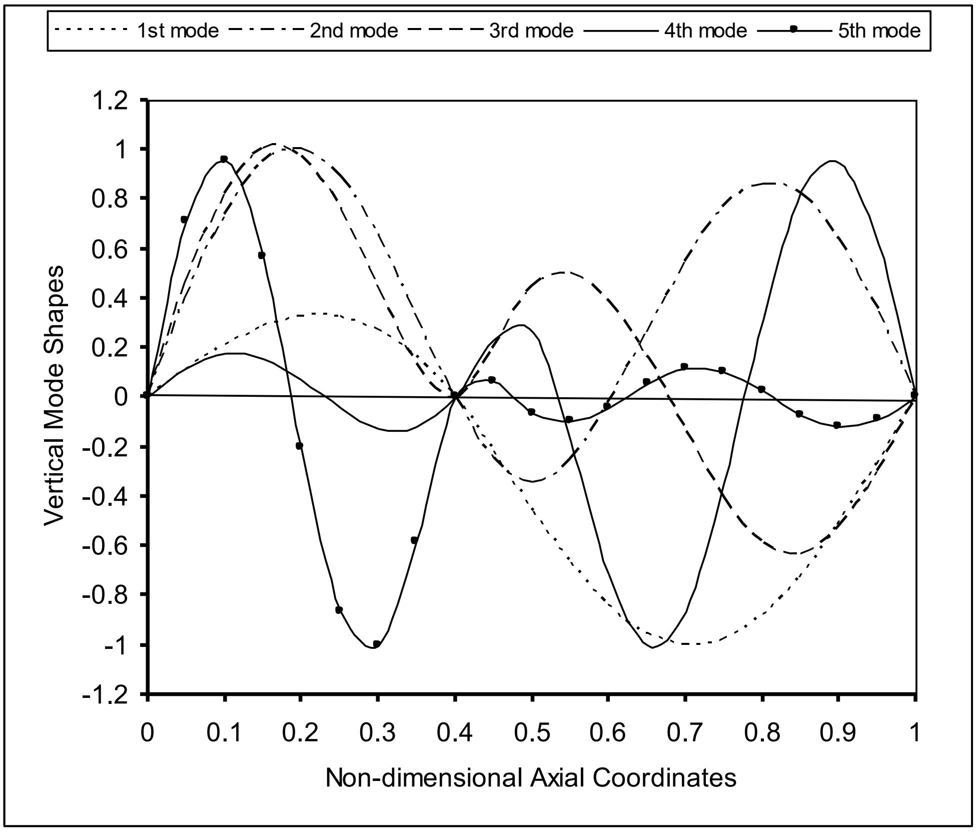

Figure 6. The first five mode shapes for the model with one intermediate point mass of two-span Timoshenko beam, $N_r = 0.75$

It can be seen from Table 6 that, as the axial compressive force acting to the beam is increased, the first five natural frequency values are decreased. From Table 6 one can sees that, the first five frequency values of Timoshenko beam increase with increasing number intermediate pinned supports for N_r is being constant.

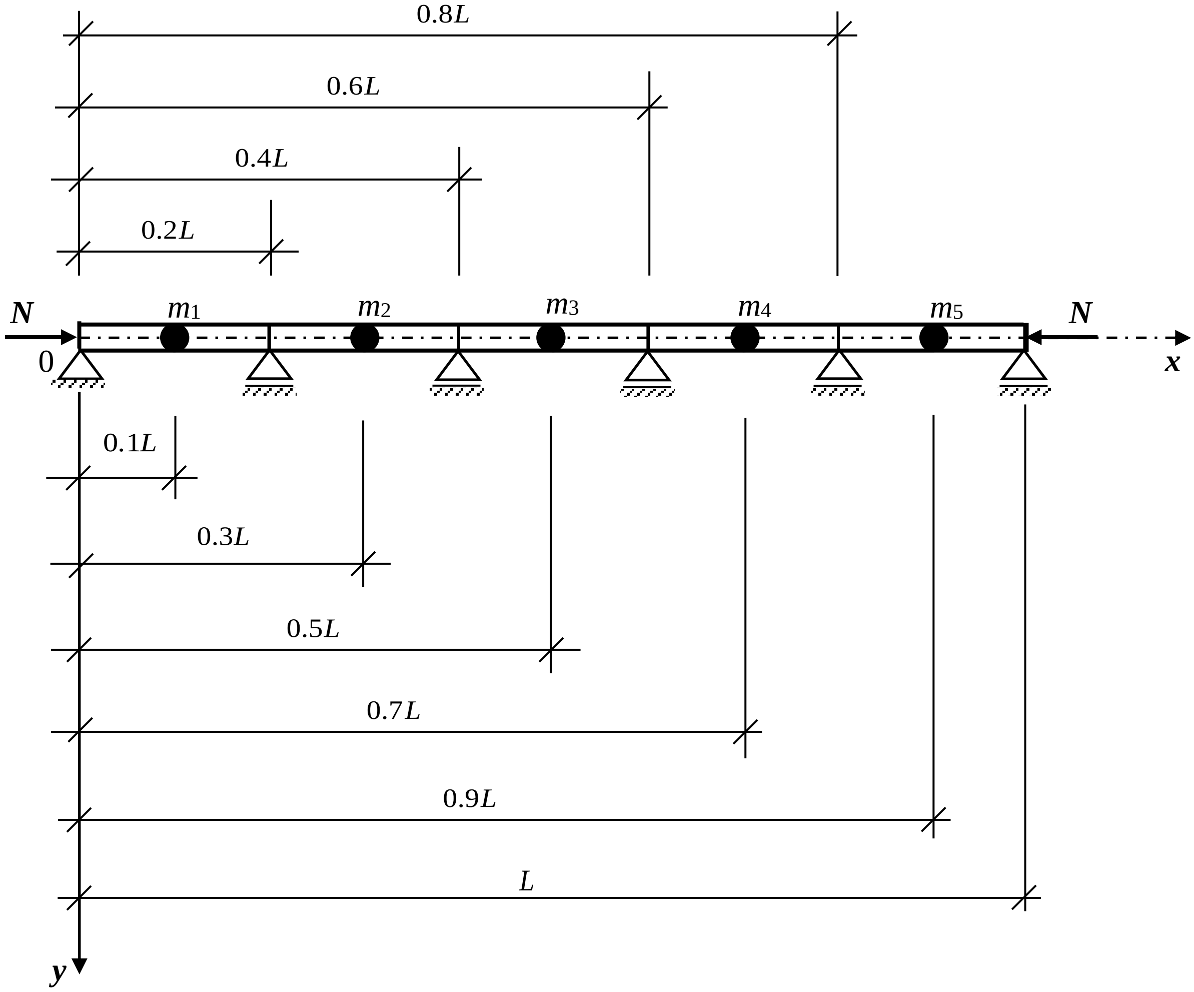

Figure 7. A pinned-pinned Timoshenko beam carrying five intermediate point masses and with multiple intermediate supports

In application of DTM, the natural frequency values of the beams are calculated by increasing series size $\bar{N}$. In Table 6, convergences of the first five natural frequencies are introduced. Here, it is seen that; for the case with one intermediate pinned support, when the series size is taken 62; for the case with two intermediate pinned supports, when the series size is taken 64 and for the case with four intermediate pinned supports, when the series size is taken 70, the natural frequency values of the fifth mode appears.

Table 6. The first five natural frequencies of the uniform pinned-pinned Timoshenko beam carrying five intermediate point masses and with multiple intermediate supports for different values of N_r

No. of supports h	Location of supports $\bar{z}_1 = \bar{x}_1/L$	ω_α (rad/sec)	METHOD	$N_r = 0.00$	$N_r = 0.25$	$N_r = 0.50$	$N_r = 0.75$
1	0.4	ω_1	DTM $(\bar{N}=38)$	1009.4985	975.9811	941.1671	904.9004
			NAT	1009.4985	975.9811	941.1670	904.9001
		ω_2	DTM $(\bar{N}=46)$	2871.5132	2830.3774	2788.4976	2745.8410
			NAT	2871.5130	2830.3776	2788.4972	2745.8398
		ω_3	DTM $(\bar{N}=52)$	3793.1357	3762.2137	3731.0649	3699.6820
			NAT	3793.1356	3762.2137	3731.0647	3699.6816
		ω_4	DTM $(\bar{N}=58)$	5990.2710	5962.1208	5933.7823	5905.2525
			NAT	5990.2710	5962.1208	5933.7822	5905.2522
		ω_5	DTM $(\bar{N}=62)$	8905.3494	8873.3926	8841.3288	8809.1559
			NAT	8905.3490	8873.3921	8841.3277	8809.1547
2	0.4 0.6	ω_1	DTM $(\bar{N}=38)$	2127.1555	2099.2842	2070.9711	2042.1948
			NAT	2127.1555	2099.2841	2070.9707	2042.1941
		ω_2	DTM $(\bar{N}=48)$	3350.9244	3309.0376	3266.5866	3223.5512
			NAT	3350.9244	3309.0376	3266.5865	3223.5500
		ω_3	DTM $(\bar{N}=54)$	5340.1176	5316.4338	5292.6119	5268.6496
			NAT	5340.1175	5316.4333	5292.6111	5268.6485
		ω_4	DTM $(\bar{N}=58)$	7769.6566	7740.2002	7710.5298	7680.6438
			NAT	7769.6567	7740.2001	7710.5294	7680.6427
		ω_5	DTM $(\bar{N}=64)$	9479.4964	9456.6222	9433.7603	9410.9113
			NAT	9479.4963	9456.6222	9433.7604	9410.9104
4	0.2 0.4 0.6 0.8	ω_1	DTM $(\bar{N}=42)$	4864.5918	4843.6994	4822.6842	4801.5457
			NAT	4864.5915	4843.6988	4822.6840	4801.5451
		ω_2	DTM $(\bar{N}=52)$	6739.7248	6716.6454	6693.4179	6670.0392
			NAT	6739.7248	6716.6453	6693.4177	6670.0392
		ω_3	DTM $(\bar{N}=58)$	8172.5070	8148.7995	8124.9158	8100.8535
			NAT	8172.5070	8148.7992	8124.9151	8100.8529
		ω_4	DTM $(\bar{N}=62)$	9414.0635	9389.1610	9364.2769	9339.4130
			NAT	9414.0632	9389.1605	9364.2765	9339.4126
		ω_5	DTM $(\bar{N}=70)$	11819.6673	11798.5832	11777.4779	11756.3515
			NAT	11819.6673	11798.5831	11777.4777	11756.3510

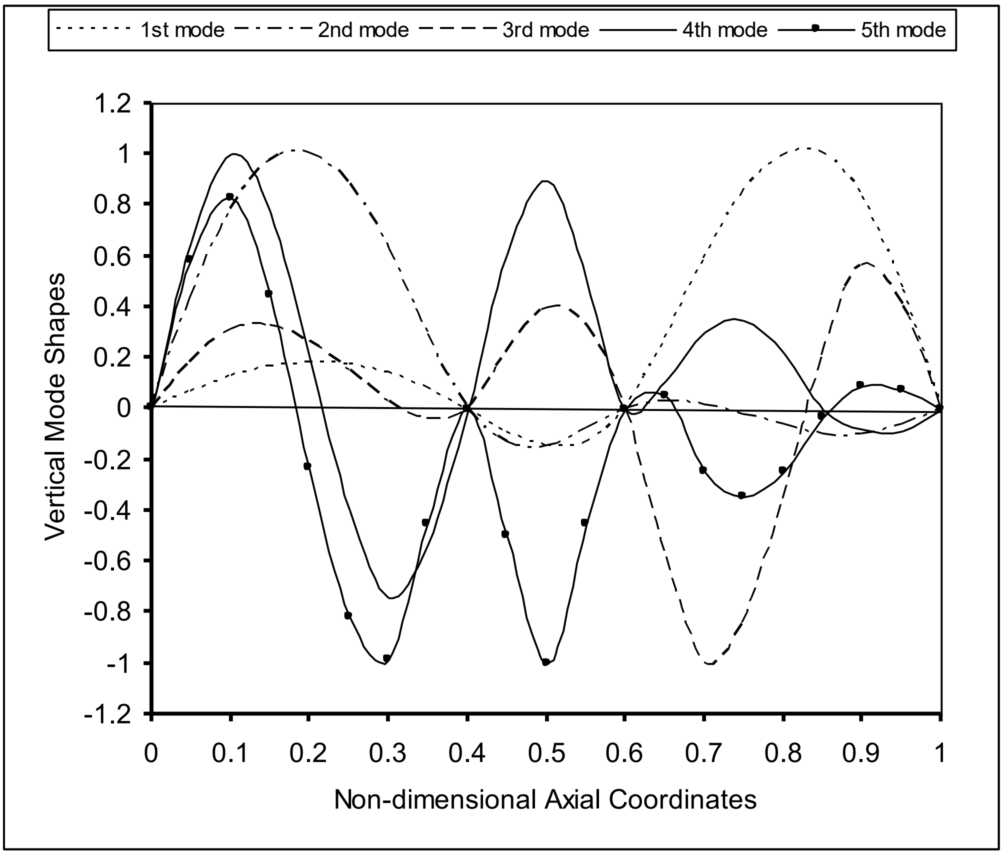

Figure 8. The first five mode shapes of pinned-pinned Timoshenko beam carrying five intermediate point masses and with two intermediate supports located at $\bar{x}_1 = 0.4L$ and $\bar{x}_2 = 0.6L$ for $N_r = 0.75$

6. CONCLUSIONS

In this study, frequency values and mode shapes for free vibration of the multi-span Timoshenko beam subjected to the axial compressive force with multiple point masses are obtained for different number of spans and point masses with different locations and for different values of axial compressive force by using DTM and NAT. In the three numerical examples, the frequency values are determined for Timoshenko beams with and without the axial force effect and are presented in the tables. The frequency values obtained for the Timoshenko beam without the axial force effect in this study are on the order of 2-5% less than the values obtained for the Bernoulli-Euler beam in [7], as expected, since the shear deformation is considered in Timoshenko beam theory. The increase in the value of axial force also causes a decrease in the frequency values.

It can be seen from the tables that the frequency values show a very high decrease as a point mass is attached to the bare beam; the amount of this decrease considerably increases as the number of point masses is increased.

The essential steps of the DTM application includes transforming the governing equations of motion into algebraic equations, solving the transformed equations and then applying a process of inverse transformation to obtain any desired natural frequency. All the steps of the DTM are very straightforward and the application of the DTM to both the equations of motion and the boundary conditions seem to be very involved computationally. However, all the algebraic calculations are finished quickly using symbolic computational software. Besides all these, the analysis of the convergence of the results show that DTM solutions converge fast. When the results of the DTM are compared with the results of NAT, very good agreement is observed.

APPENDIX

From Eqs.(2), (3), (4) and (5), the boundary conditions for the p^{th} intermediate point mass can be written in matrix equation form as:

$$\left[B_{p'}\right] \cdot \left\{C_{p'}\right\} = \{0\} \tag{A.1}$$

where

$$\left\{C_{p'}\right\}^T = \left\{C_{p'-1,1} \quad C_{p'-1,2} \quad C_{p'-1,3} \quad C_{p'-1,4} \quad C_{p',1} \quad C_{p',2} \quad C_{p',3} \quad C_{p',4}\right\} \tag{A.2}$$

$$\left[B_{p'}\right] = \begin{array}{c} \begin{array}{cccccccc} 4p'-3 & 4p'-2 & 4p'-1 & 4p' & 4p'+1 & 4p'+2 & 4p'+3 & 4p'+4 \end{array} \\ \left[\begin{array}{cccccccc} ch_1 & sh_1 & cs_2 & sn_2 & -ch_1 & -sh_1 & -cs_2 & -sn_2 \\ K_3 \cdot sh_1 & K_3 \cdot ch_1 & K_4 \cdot sn_2 & -K_4 \cdot cs_2 & -K_3 \cdot sh_1 & -K_3 \cdot ch_1 & -K_4 \cdot sn_2 & K_4 \cdot cs_2 \\ K_1 \cdot ch_1 & K_1 \cdot sh_1 & -K_2 \cdot cs_2 & -K_2 \cdot sn_2 & -K_1 \cdot ch_1 & -K_1 \cdot sh_1 & K_2 \cdot cs_2 & K_2 \cdot sn_2 \\ K_5 \cdot sh_1 + \alpha_1 & K_5 \cdot ch_1 + \alpha_2 & K_6 \cdot sn_2 + \alpha_3 & -K_6 \cdot cs_2 + \alpha_4 & -K_5 \cdot sh_1 & -K_5 \cdot ch_1 & -K_6 \cdot sn_2 & K_6 \cdot cs_2 \end{array}\right] \end{array} \begin{array}{c} \\ 4p'-1 \\ 4p' \\ 4p'+1 \\ 4p'+2 \end{array} \tag{A.3}$$

$ch_1 = \cosh\left(D_1 \cdot z_{p'}\right)$; $ch_2 = \cosh\left(D_2 \cdot z_{p'}\right)$; $sh_1 = \sinh\left(D_1 \cdot z_{p'}\right)$; $sh_2 = \sinh\left(D_2 \cdot z_{p'}\right)$;

$cs_1 = \cos\left(D_1 \cdot z_{p'}\right)$; $cs_2 = \cos\left(D_2 \cdot z_{p'}\right)$; $sn_1 = \sin\left(D_1 \cdot z_{p'}\right)$; $sn_2 = \sin\left(D_2 \cdot z_{p'}\right)$;

$K_5 = \frac{AG}{\bar{k}} \cdot \left(\frac{D_1}{L} - K_3\right)$; $K_6 = \frac{AG}{\bar{k}} \cdot \left(-\frac{D_2}{L} - K_4\right)$; $\alpha_1 = m_p \cdot \omega^2 \cdot ch_1$; $\alpha_2 = m_p \cdot \omega^2 \cdot sh_1$

$\alpha_3 = m_p \cdot \omega^2 \cdot cs_2$; $\alpha_4 = m_p \cdot \omega^2 \cdot sn_2$

From Eqs.(2), (3), and (4), the boundary conditions for the r^{th} intermediate support can be written in matrix equation form as:

$$\left[B_{r'}\right] \cdot \left\{C_{r'}\right\} = \{0\} \tag{A.4}$$

where

$$\left\{C_{r'}\right\}^T = \left\{C_{r'-1,1} \quad C_{r'-1,2} \quad C_{r'-1,3} \quad C_{r'-1,4} \quad C_{r',1} \quad C_{r',2} \quad C_{r',3} \quad C_{r',4}\right\} \tag{A.5}$$

$$\left[B_{r'}\right]=\begin{array}{cc} \begin{array}{cccccccc} 4r'-3 & 4r'-2 & 4r'-1 & 4r' & 4r'+1 & 4r'+2 & 4r'+3 & 4r'+4 \end{array} & \\ \begin{bmatrix} chr_1 & shr_1 & csr_2 & snr_2 & 0 & 0 & 0 & 0 \\ 0 & 0 & 0 & 0 & chr_1 & shr_1 & csr_2 & snr_2 \\ K_3\cdot shr_1 & K_3\cdot chr_1 & K_4\cdot snr_2 & -K_4\cdot csr_2 & -K_3\cdot shr_1 & -K_3\cdot chr_1 & -K_4\cdot snr_2 & K_4\cdot csr_2 \\ K_1\cdot chr_1 & K_1\cdot shr_1 & -K_2\cdot csr_2 & -K_2\cdot snr_2 & -K_1\cdot chr_1 & -K_1\cdot shr_1 & K_2\cdot csr_2 & K_2\cdot snr_2 \end{bmatrix} & \begin{array}{c} 4r'-1 \\ 4r' \\ 4r'+1 \\ 4r'+2 \end{array} \end{array}$$

(A.6)

$$chr_1=\cosh\left(D_1\cdot z_{r'}\right)\;;\;\; chr_2=\cosh\left(D_2\cdot z_{r'}\right)\;;\;\; shr_1=\sinh\left(D_1\cdot z_{r'}\right)\;;\;\; shr_2=\sinh\left(D_2\cdot z_{r'}\right)$$

$$csr_1=\cos\left(D_1\cdot z_{r'}\right)\;;\;\; csr_2=\cos\left(D_2\cdot z_{r'}\right)\;;\;\; snr_1=\sin\left(D_1\cdot z_{r'}\right)\;;\;\; snr_2=\sin\left(D_2\cdot z_{r'}\right)$$

REFERENCES

[1] Liu WH, Wu JR, Huang CC. Free Vibration Of Beams With Elastically Restrained Edges And Intermediate Concentrated Masses, *Journal of Sound and Vibration*, Cilt.122, 1998, s.193-207.

[2] Wu JS, Chou HM., A New Approach For Determining The Natural Frequencies And Mode Shape Of A Uniform Beam Carrying Any Number Of Spring Masses, *Journal of Sound and Vibration*, Cilt.220, 1999, s.451-468.

[3] Gürgöze M, Erol, H., Determination Of The Frequency Response Function Of A Cantilever Beam Simply Supported In-Span, *Journal of Sound and Vibration*, Cilt.247, 2001, s.372-378.

[4] Gürgöze M, Erol H., On The Frequency Response Function Of A Damped Cantilever Beam Simply Supported In-Span And Carrying A Tip Mass, *Journal of Sound and Vibration*, Cilt.255, 2002, s.489-500.

[5] Naguleswaran S. Transverse Vibrations Of An Euler-Bernoulli Uniform Beam Carrying Several Particles, *International Journal of Mechanical Science*, Cilt.44, 2002, s.2463-2478.

[6] Naguleswaran S. Transverse Vibration Of An Euler-Bernoulli Uniform Beam On Up O Five Resilient Supports Including Ends, *Journal of Sound and Vibration*, Cilt.261, 2003, s.372-384.

[7] Lin HY, Tsai YC. On The Natural Frequencies And Mode Shapes Of A Uniform Multi-Span Beam Carrying Multiple Point Masses, *Structural Engineering and Mechanics*, Cilt.21, 2005, s.351-367.

[8] Lin HY, Tsai YC. On The Natural Frequencies And Mode Shapes Of A Multiple-Step Beam Carrying A Number Of Intermediate Lumped Masses And Rotary Inertias, *Structural Engineering and Mechanics*, Cilt.22, 2006, s.701-717.

[9] Lin HY, Tsai YC. Free Vibration Analysis Of A Uniform Multi-Span Beam Carrying Multiple Spring-Mass Systems, *Journal of Sound and Vibration*, Cilt.302, 2007, s.442-456.

[10] Wang JR, Liu TL, Chen DW. Free Vibration Analysis Of A Timoshenko Beam Carrying Multiple Spring-Mass Systems With The Effects Of Shear Deformation And Rotatory Inertia, *Structural Engineering and Mechanics*, Cilt.26, 2007, s.1-14.

[11] Yesilce Y, Demirdag O, Catal S. Free Vibrations Of A Multi-Span Timoshenko Beam Carrying Multiple Spring-Mass Systems, *Sadhana*, Cilt.33, 2008, s.385-401.

[12] Yesilce Y, Demirdag O. Effect Of Axial Force On Free Vibration Of Timoshenko Multi-Span Beam Carrying Multiple Spring-Mass Systems, *International Journal of Mechanical Science*, Cilt.50, 2008, s.995-1003.
[13] Lin HY. Dynamic Analysis Of A Multi-Span Uniform Beam Carrying A Number Of Various Concentrated Elements, *Journal of Sound and Vibration*, Cilt.309, 2008, s.262-275.
[14] Yesilce Y. Effect Of Axial Force On The Free Vibration Of Reddy-Bickford Multi-Span Beam Carrying Multiple Spring-Mass Systems, *Journal of Vibration and Control*, Cilt.16, 2010, s.11-32.
[15] Lin HY. An Exact Solution For Free Vibrations Of A Non-Uniform Beam Carrying Multiple Elastic-Supported Rigid Bars, *Structural Engineering and Mechanics*, Cilt.34, 2010, s.399-416.
[16] Zhou JK. *Differential transformation and its applications for electrical circuits*, Wuhan China: Huazhong University Press, 1986.
[17] Ozgumus OO, Kaya MO. Flapwise Bending Vibration Analysis Of Double Tapered Rotating Euler-Bernoulli Beam By Using The Differential Transform Method, *Meccanica*, Cilt.41, 2006, s.661-670.
[18] Çatal S. Analysis Of Free Vibration Of Beam On Elastic Soil Using Differential Transform Method, *Structural Engineering and Mechanics*, Cilt.24, 2006, s.51-62.
[19] Çatal S. Solution Of Free Vibration Equations Of Beam On Elastic Soil By Using Differential Transform Method, *Applied Mathematical Modelling*, Cilt.32, 2008, s.1744-1757.
[20] Çatal S, Çatal, HH., Buckling Analysis Of Partially Embedded Pile İn Elastic Soil Using Differential Transform Method, *Structural Engineering and Mechanics*, Cilt.24, 2006, s.247-268.
[21] Ozgumus OO, Kaya MO., Energy Expressions And Free Vibration Analysis Of A Rotating Double Tapered Timoshenko Beam Featuring Bending-Torsion Coupling, *International Journal of Engineering Science*, Cilt.45, 2007, s.562-586.
[22] Kaya MO, Ozgumus OO. Flexural-Torsional-Coupled Vibration Analysis Of Axially Loaded Closed-Section Composite Timoshenko Beam By Using DTM, *Journal of Sound and Vibration*, Cilt.306, 2007, s.495-506.
[23] Yesilce Y, Catal S., Free Vibration Of Axially Loaded Reddy-Bickford Beam On Elastic Soil Using The Differential Transform Method, *Structural Engineering and Mechanics*, Cilt.31, 2009, s.453-476.

CV/ÖZGEÇMİŞ

Yusuf YEŞİLCE; Associate Prof. (Doç. Dr.)

He got his bachelors' degree in Civil Engineering Department at Dokuz Eylul University in 2002, his master degree in Structural Engineering MSc program at Dokuz Eylul University in 2005 and his PhD degree in Structural Engineering PhD program at Dokuz Eylul University in 2009. He is an academic member of Civil Engineering Department of Dokuz Eylul University. His research interests focus on static and dynamic analysis of structures and structural mechanics.

Lisans derecesini 2002'de Dokuz Eylül Üniversitesi İnşaat Mühendisliği Bölümü'nden, yüksek lisans derecesini 2005'de Dokuz Eylül Üniversitesi Yapı Programı'ndan ve doktora derecesini 2009'da Dokuz Eylül Üniversitesi Yapı Doktora Programı'ndan aldı. Dokuz Eylül Üniversitesi Mühendislik Fakültesi İnşaat Mühendisliği Bölümü'nde öğretim üyesi olarak görev yapmaktadır. Araştırma ve çalışma alanları yapıların statik ve dinamik analizi ve yapı mekaniği üzerinedir.